HAYATI
Journal of Biosciences

Vol. 33 No. 6, November 2026 1441-1450
DOI:10.4308/hjb.33.6.1441-1450
ISSN: 1978-3019
EISSN: 2086-4094

Research Article

Check for updates

OPEN ACCESS

Functional Screening and Biochemical Correlates of *Streptomyces* Antagonism Against *Fusarium* sp.

Lan-Phuong Ly[1,2], Huu-Thanh Nguyen[2,3], Phu-Tho Nguyen[2,3]*

[1]*Graduate University of Science and Technology, Vietnam Academy of Science and Technology, Ha Noi, Vietnam*
[2]*Faculty of Agriculture and Natural Resources, An Giang University, An Giang, Vietnam*
[3]*Vietnam National University, Ho Chi Minh City, Vietnam*

ARTICLE INFO

Article history:
Received June 2, 2026
Received in revised form August 4, 2026
Accepted September 23, 2026
Available Online October 6, 2026

KEYWORDS:
Antifungal activity,
chitinase,
functional screening,
Fusarium,
Streptomyces

Copyright (c) 2026 @author(s).

ABSTRACT

Although antagonistic *Streptomyces* are widely recognized for their antifungal potential, trait-based selection of effective isolates remains insufficiently explored. In this study, we recovered thirty-eight *Streptomyces*-like actinomycete isolates from agricultural soils and screened them for antifungal activity against *Fusarium* sp. using a dual-culture assay. We further evaluated antagonistic isolates for chitinase activity, total protein content, and Folin–Ciocalteu-reactive phenolic-equivalent content. We conducted correlation analyses to examine associations between these biochemical traits and fungal growth inhibition. Sixteen isolates (42%) exhibited antifungal activity, with inhibition values ranging from 1.84 to 69.20%, while isolates VAS10 and VAS35 achieved at least 65% suppression. Among the measured traits, chitinase activity showed the strongest positive association with fungal growth inhibition, followed by Folin–Ciocalteu-reactive phenolic-equivalent content. In contrast, total protein content was not significantly associated with inhibition. These results suggest that chitinase activity may serve as a preliminary screening indicator associated with antifungal performance; however, the correlation analysis and limited biochemical measurements do not establish causality or define the underlying antifungal mechanism. Accordingly, the present findings support the prioritization of VAS10 and VAS35 for further validation but do not demonstrate their efficacy *in planta* or establish them as validated biocontrol agents.

1. Introduction

Soil-borne fungal diseases represent a major constraint to crop productivity worldwide, particularly in intensive vegetable production systems (Hossain *et al.* 2025). Among these pathogens, *Fusarium* species cause severe vascular wilt diseases, leading to significant yield losses and reduced crop quality (Li *et al.* 2025). *Fusarium*-induced wilt is especially problematic because of the pathogen survives long-term in soil and can infect hosts across multiple developmental stages (Sarnaik *et al.* 2025). In recent years, climate change, intensified monocropping, and increased global movement of plant materials have further increased the incidence and severity of soil-borne fungal diseases, particularly in tropical and subtropical regions (Islam *et al.* 2024; Li *et al.* 2025). Conventional disease management strategies still rely heavily on chemical fungicides; however, their extensive and prolonged use has raised serious concerns about environmental contamination, pathogen resistance, and adverse effects on non-target organisms (Islam *et al.* 2024). These limitations have spurred growing interest in sustainable, environmentally friendly alternatives for disease control (Hossain *et al.* 2025).

Biological control using antagonistic microorganisms has emerged as a promising approach for managing soil-borne plant pathogens and reducing reliance on chemical fungicides (Todorović *et al.* 2023). Among beneficial microbes, members of the

* Corresponding Author
E-mail Address: nptho@agu.edu.vn

genus *Streptomyces* are of particular interest because of their well-documented capacity to produce antifungal enzymes and a wide array of secondary metabolites (Van der Meij *et al.* 2017). Previous studies have demonstrated that *Streptomyces* spp. suppress *Fusarium* growth through multiple mechanisms, including the production of hydrolytic enzymes such as chitinases, synthesis of antifungal compounds, and competition for nutrients and ecological niches (Pacios-Michelena *et al.* 2021). Recent advances in microbial ecology and genomics have further highlighted the ecological adaptability and functional diversity of *Streptomyces* spp., supporting their persistence and activity in complex soil environments (Mispelaere *et al.* 2024).

Despite extensive reports on the antifungal potential of Streptomyces, the relationship between specific biochemical traits and effective disease suppression remains insufficiently understood (Khan *et al.* 2023). In particular, the relationships of chitinase activity, total protein content, and Folin–Ciocalteu-reactive phenolic-equivalent content with antifungal performance may vary considerably among isolates and environmental conditions (Khan *et al.* 2023; Davidova *et al.* 2024). Recent studies have emphasized that antifungal efficacy cannot be reliably inferred from individual biochemical parameters alone, underscoring the need for integrative analyses that link biochemical traits with biological outcomes. Although genomic and comparative studies have improved our understanding of functional diversity within *Streptomyces*, comprehensive investigations integrating biochemical characterization, molecular identification, and correlation analysis of antifungal performance remain limited, particularly in *Fusarium* pathosystems (Mispelaere *et al.* 2024).

Therefore, the objective of the present study was to isolate and screen soil-derived *Streptomyces*-like actinomycetes for antifungal activity against *Fusarium* sp., quantify selected extracellular biochemical traits, including chitinase activity, total protein content, and Folin–Ciocalteu-reactive phenolic-equivalent content, and examine their statistical associations with antifungal inhibition. The most effective isolates were further identified at the genus level using 16S rRNA gene sequencing. This study was a functional screening and correlation analysis and did not aim to identify individual antifungal metabolites or establish a metabolite-specific mechanism of action. By integrating *in vitro* antagonism assays, selected extracellular biochemical measurements, and molecular identification, this study provides a functional framework for prioritizing *Streptomyces* isolates for subsequent antifungal and in planta validation.

2. Materials and Methods

2.1. Soil Sampling

Soil samples were collected from agricultural fields in An Giang province, Vietnam, during the dry season. Sampling sites were selected based of ongoing agricultural use and the availability of representative rhizosphere/topsoil sampling points. Composite soil samples were obtained from the rhizosphere/topsoil layer at a depth of approximately 0–15 cm. Each composite sample consisted of five subsamples collected randomly within the same site to ensure representative sampling. Soil samples were placed in sterile polyethylene bags, transported to the laboratory under ambient conditions, and processed within 24 h of collection to minimize changes in microbial composition.

2.2. Isolation of *Streptomyces*-Like Actinomycete Isolates from Soil

We obtained actinomycete-like isolates with *Streptomyces*-type colony morphology using serial dilution plating. Briefly, 10 g of each soil sample was suspended in 90 mL of sterile saline solution (0.85% NaCl) and homogenized by shaking at 150 rpm for 30 min. The suspension was serially diluted up to 10^{-5}, and 100 µL aliquots from appropriate dilutions were spread onto Gause's No. 1 agar medium (soluble starch 20.0 g/L, KNO_3 1.0 g/L, NaCl 0.5 g/L, K_2HPO_4 0.5 g/L, $MgSO_4 \cdot 7H_2O$ 0.5 g/L, $FeSO_4 \cdot 7H_2O$ 0.01 g/L; agar 20.0 g/L; pH 7.3) for primary isolation of actinomycete-like colonies (Zhang *et al.* 2026). Plates were incubated at 28–30°C for 7–10 d. Colonies exhibiting typical Streptomyces-like morphology, including a dry or chalky appearance and pigmented aerial mycelia, were selected and purified by repeated streaking on the same medium until pure cultures were obtained. We coded pure isolates and maintained them on Gause's No. 1 agar slants at 4°C for short-term storage and preserved them in 20% (v/v) glycerol stocks at −80°C for long-term storage.

Following purification, the isolates were point-inoculated onto fresh Gause's No. 1 agar plates and incubated at 28–30°C for 96 h. Macroscopic colony characteristics, including colony color, surface appearance, margin, and elevation, were then recorded, and representative colonies were photographed. These observations served as preliminary phenotypic

characterization, while taxonomic assignment of the two most active isolates was supported by 16S rRNA gene sequencing.

2.3. Primary Screening for Antifungal Activity against *Fusarium*

The antifungal activity of putative *Streptomyces* isolates was evaluated using a dual-culture assay on potato dextrose agar (PDA), following Amini *et al.* (2016) with minor modifications. The fungal isolate used as the target pathogen was obtained from our previous work and maintained in the laboratory. Its ITS sequence had previously been generated and deposited in GenBank under accession no. PX745173.1. Additional sequence comparison based on the EF-1α/TEF-1α region supported its putative assignment to *Fusarium hainanense*. In this study, the isolate was used as the representative *Fusarium* sp. target for antifungal screening.

A 5-mm mycelial plug taken from the actively growing margin of a 5-day-old *Fusarium* culture was placed at the center of each PDA plate. Each putative *Streptomyces* isolate was inoculated at four equidistant points surrounding the fungal plug, approximately 25 mm from the center. Control plates contained only the fungal plug. Plates were incubated at 28°C for 96 h, after which radial fungal growth was measured along four perpendicular axes and averaged for each plate. Antifungal inhibition was calculated as inhibition (%) = 100 × (Rc − Rt) / Rc, where Rc is the mean radial growth of the fungus on control plates, and Rt is the mean radial growth in the presence of the *Streptomyces* isolate. Isolates showing measurable inhibition were considered antagonistic and were selected for subsequent biochemical analyses.

2.4. Preparation of Cell-Free Culture Supernatants and Measurement of Selected Extracellular Biochemical Traits

Antagonistic isolates were cultivated in the corresponding liquid formulation of Gause's No. 1 medium under shaking conditions (30°C, 180 rpm) for 7 d. Following incubation, cultures were centrifuged at 8,000 × g for 10 min to remove cells and mycelia. We collected the resulting cell-free culture supernatants of measure selected extracellular biochemical traits. We conducted all assays using three independent biological replicates. Biochemical measurements were expressed on a culture-volume basis per milliliter of cell-free culture supernatant and were not normalized to culture biomass, dry cell weight, or optical density. Therefore, the reported values represent volumetric extracellular activities or concentrations under the culture conditions used rather than biomass-specific production. We determined chitinolytic activity in the cell-free culture supernatants, operationally reported as chitinase activity under the specified assay conditions, using a colloidal chitin-based assay. We quantified the released reducing sugars colorimetrically using the 3,5-dinitrosalicylic acid method, with N-acetylglucosamine as the standard (Subramanian *et al.* 2020). One unit of chitinase activity was defined as the amount of enzyme required to release 1 µmol of reducing sugar per minute under assay conditions. Total protein content was quantified using a colorimetric Bradford assay with bovine serum albumin as the standard (Bradford 1976). Folin–Ciocalteu-reactive phenolic-equivalent content was determined using the Folin–Ciocalteu method with gallic acid as the standard, and results were expressed as µg gallic acid equivalents per mL (µg GAE/mL) (Dominguez-López *et al.* 2024). These assays were intended as comparative screening measurements of selected extracellular traits. They did not evaluate enzyme specificity toward alternative substrates, enzyme or metabolite stability, extracellular metabolite composition, or production kinetics over the course of cultivation.

2.5. Molecular Identification of Selected Isolates Based on 16S rRNA Gene Sequencing

We selected two isolates with the strongest antifungal activity for molecular identification. We extracted genomic DNA from bacterial biomass using a standard bacterial DNA extraction protocol. The 16S rRNA gene was amplified by polymerase chain reaction (PCR) using universal primers 27F and 1492R, covering a nearly full-length region of the 16S rRNA gene (Palkova *et al.* 2021). PCR products were verified by agarose gel electrophoresis, purified, and subjected to Sanger sequencing. The obtained 16S rRNA gene sequences were compared with sequences available in the NCBI nucleotide database using BLASTn. The nearly full-length 16S rRNA gene sequences of *Streptomyces* sp. VAS10 and *Streptomyces* sp. VAS35 were deposited in GenBank under accession numbers PZ770648 and PZ770649, respectively. Closely related and taxonomically relevant reference sequences were selected from GenBank based on BLASTn results. Sequences were aligned using MUSCLE in MEGA 12, and non-overlapping terminal regions were removed.

The maximum-likelihood tree was reconstructed using the best-fit HKY+I model selected according to the Bayesian information criterion. Complete deletion was applied, resulting in 1,336 aligned positions, and branch support was assessed using 1,000 standard bootstrap replicates. We used *Kitasatospora herbariicolor* NRRL B-3299T (NR_115776.1) as the outgroup.

2.6. Statistical Analysis

All experiments were conducted with three independent biological replicates, and results were expressed as mean ± standard deviation. Normality of model residuals and homogeneity of variances were assessed separately for each response variable using the Shapiro–Wilk test and the Brown–Forsythe test (median-centered Levene test), respectively. Variables satisfying both assumptions were analyzed using one-way ANOVA followed by Duncan's multiple range test. Variables showing significant departures from normality were analyzed using the Kruskal–Wallis test followed by Dunn's multiple-comparison test with Holm adjustment. Pearson correlation analysis was used to evaluate associations between antifungal inhibition and the measured extracellular biochemical traits.

3. Results

3.1. Isolation and Primary Screening of *Streptomyces*-Like Actinomycete Isolates

A total of 38 actinomycete-like isolates with Streptomyces-type morphology were recovered from agricultural soil samples. Colony morphology on Gause's No. 1 agar revealed clear phenotypic diversity among the isolates, which were grouped into 13 colony morphotypes based on colony color, surface appearance, margin, and elevation (Table 1). Colony colors included ivory-white, opaque white, cream–pale yellow, yellowish cream, milky white, yellowish white, pale yellow, and pale orange. Surface appearances included smooth, velvety, powdery, cottony, dry, rough, and wrinkled forms, whereas colony margins ranged from entire to filamentous, fimbriate, lobate, undulate, diffuse, or irregular. Most isolates formed raised colonies, while seven isolates exhibited flat colonies. Gram staining showed that the recovered isolates were Gram-positive. Together with their colony characteristics, these observations supported their preliminary classification as *Streptomyces*-like actinomycetes, while 16S rRNA

Table 1. Colony morphotypes of *Streptomyces*-like actinomycete isolates recovered from agricultural soils on Gause's No. 1 agar

Morphotype	Colony color	Surface appearance	Margin	Elevation	Representative isolates	No. of isolates
M1	Ivory-white	Velvety to wrinkled	Filamentous to lobate	Raised	VAS1, VAS6, VAS8, VAS21, VAS36, VAS63	6
M2	Ivory-white	Smooth	Entire	Flat	VAS7	1
M3	Cream–pale yellow	Velvety to powdery, radially furrowed	Filamentous to fimbriate	Raised	VAS10, VAS18, VAS27, VAS28, VAS30, VAS43, VAS46, VAS49, VAS67	9
M4	Opaque white	Smooth	Entire	Flat	VAS4, VAS14	2
M5	Yellowish cream	Wrinkled to powdery	Lobate to filamentous	Raised	VAS5, VAS25, VAS26, VAS55, VAS68, VAS69	6
M6	Milky white	Dry, rough, and wrinkled	Undulate to irregular	Flat	VAS22, VAS24	2
M7	Ivory-white	Velvety to powdery, radially furrowed	Filamentous	Raised	VAS23, VAS35	2
M8	Yellowish white	Velvety, radially striated	Filamentous to irregular	Raised	VAS53	1
M9	Pale yellow	Smooth	Entire	Raised	VAS11, VAS32, VAS41, VAS52, VAS72	5
M10	Pale orange	Smooth	Entire	Raised	VAS3	1
M11	Pale yellow–milky white	Cottony to velvety	Diffuse to irregular	Flat	VAS19	1
M12	Pale yellow–opaque white	Wrinkled, concentrically zoned	Lobate to irregular	Flat	VAS70	1
M13	Ivory-white	Velvety to powdery	Diffuse to filamentous	Raised	VAS45	1

Morphotypes were defined based on colony color, surface appearance, margin, and elevation after 96 h of incubation on Gause's No. 1 agar at 28–30°C. All isolates exhibited a Gram-positive reaction under light microscopy. We used these characteristics only for preliminary phenotypic grouping

gene sequencing later supported the genus-level assignment of VAS10 and VAS35.

Primary dual-culture screening against the tested *Fusarium* isolate (GenBank accession no. PX745173.1) revealed that 16 of the 38 isolates (42%) exhibited measurable antagonistic activity and were therefore selected for further analyses. Quantitative assessment of fungal growth inhibition demonstrated substantial variability among the antagonistic isolates (Figure 1A). Inhibition values ranged from 1.84 to 69.20%, indicating marked heterogeneity in antifungal performance among the recovered putative *Streptomyces* isolates. Isolate VAS10 exhibited the strongest antifungal activity, achieving 69.20% inhibition of fungal growth, followed by VAS35 (67.33%) and VAS6 (61.24%). In contrast, several isolates displayed only marginal inhibitory effects, particularly VAS25 and VAS23, which showed less than 5% inhibition. The Kruskal–Wallis test indicated significant differences in antifungal inhibition among the isolates ($p<0.05$). Pairwise comparisons were subsequently performed

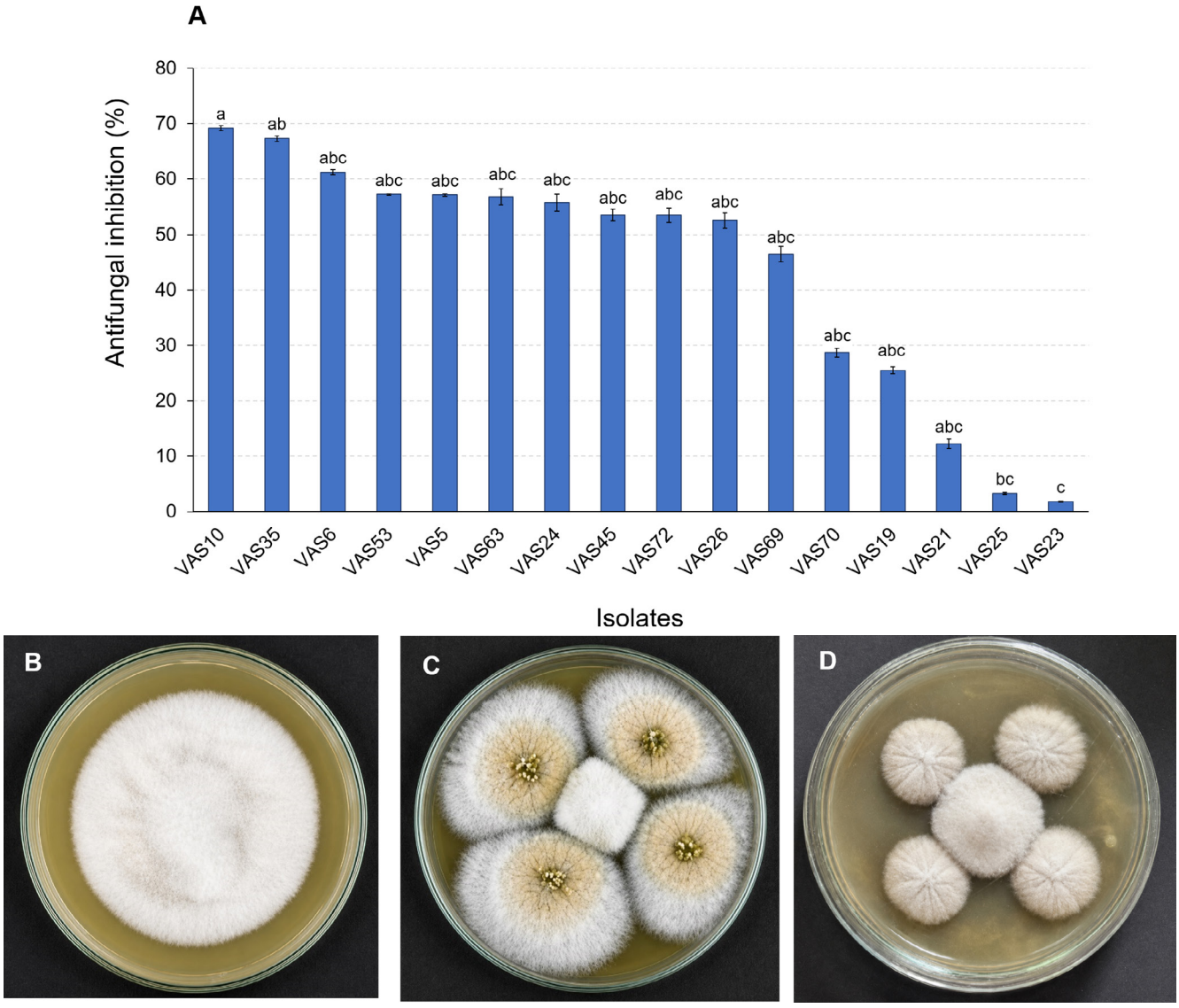


Figure 1. Antifungal activity of *Streptomyces*-like actinomycete isolates against *Fusarium* sp. (A) Quantitative inhibition of fungal growth. Values are presented as mean ± standard deviation from three independent biological replicates (n = 3). Bars sharing at least one lowercase letter are not significantly different. In contrast, bars with no letter in common differ significantly according to the Kruskal–Wallis test followed by Dunn's multiple-comparison test with Holm adjustment at $p<0.05$. Representative photographs recorded after 96 h of incubation show (B) the Fusarium-only control, (C) dual culture with *Streptomyces* sp. VAS10, and (D) dual culture with *Streptomyces* sp. VAS35. The photographs illustrate restricted fungal colony expansion in the presence of VAS10 and VAS35 relative to the control

using Dunn's test with Holm adjustment. Based on these results, isolates demonstrating high inhibition levels were prioritized for subsequent biochemical and molecular characterization.

Representative dual-culture photographs supported the quantitative inhibition results. In the *Fusarium*-only control, the fungal colony expanded broadly across the agar surface. In contrast, fungal colony expansion was markedly restricted in the presence of VAS10 and VAS35, with altered radial growth at the confrontation region (Figure 1B–D). These observations were qualitative and were not used to infer direct overgrowth, hyphal damage, or mycoparasitism.

3.2. Selected Extracellular Biochemical Traits of Antagonistic *Streptomyces*-Like Actinomycete Isolates

Table 2 summarizes selected extracellular biochemical measurements from the cell-free culture supernatants of the 16 antagonistic isolates. Isolates showed considerable variation in chitinase activity, total protein content, and Folin–Ciocalteu-reactive phenolic-equivalent content. Chitinase activity ranged from 0.30 to 0.88 U/mL across the tested isolates. Isolate VAS10 exhibited the highest chitinase activity (0.88±0.06 U/mL), followed by VAS72 (0.82±0.01 U/mL) and VAS53 (0.80±0.07 U/mL). In contrast, isolate VAS21 displayed the lowest chitinase activity (0.30±0.04 U/mL). Overall, isolates with higher antifungal activity in the primary screening tended to show higher chitinase activity.

Table 2. Selected extracellular biochemical measurements in cell-free culture supernatants of antagonistic *Streptomyces*-like actinomycete isolates

Isolate	Chitinase activity (U/mL)	Total protein (µg/mL)	Folin–Ciocalteu-reactive phenolic-equivalent content (µg GAE/mL)
VAS5	0.63±0.07^{cd}	51.67±0.42^{abc}	6.63±0.21^{f}
VAS6	0.61±0.01^{cd}	57.25±0.42^{abc}	8.01±0.44^{de}
VAS10	0.88±0.06^{a}	63.38±0.21^{a}	8.23±0.55^{de}
VAS19	0.41±0.06^{fgh}	54.75±2.08^{abc}	5.26±0.58^{g}
VAS21	0.30±0.04^{h}	47.04±2.29^{abc}	5.98±0.51^{fg}
VAS23	0.44±0.14^{efg}	43.53±2.55^{abc}	3.83±0.13^{h}
VAS24	0.61±0.01^{cd}	53.13±0.63^{abc}	5.70±0.22^{g}
VAS25	0.38±0.08^{gh}	26.52±0.23^{abc}	4.46±0.35^{h}
VAS26	0.78±0.03^{ab}	49.67±2.08^{abc}	8.40±0.35^{d}
VAS35	0.54±0.07^{de}	38.92±4.17^{abc}	12.36±0.02^{a}
VAS45	0.55±0.02^{d}	58.08±0.42^{ab}	10.24±0.14^{c}
VAS53	0.80±0.07^{ab}	24.21±0.63^{abc}	7.62±0.62^{e}
VAS63	0.72±0.09^{bc}	7.67±1.04^{c}	11.28±0.39^{b}
VAS69	0.52±0.03^{def}	16.04±2.08^{bc}	5.43±0.60^{g}
VAS70	0.38±0.03^{gh}	21.78±1.06^{abc}	4.36±0.24^{h}
VAS72	0.82±0.01^{ab}	28.46±1.04^{abc}	7.92±0.48^{de}

Values are presented as mean ± SD from three independent biological replicates (n = 3). Within each column, values sharing at least one lowercase superscript letter are not significantly different, whereas means with no letter in common differ significantly at $p < 0.05$. Chitinase activity and Folin–Ciocalteu-reactive phenolic-equivalent content were analyzed using one-way ANOVA followed by Duncan's multiple range test. Total protein content was analyzed using the Kruskal–Wallis test followed by Dunn's multiple-comparison test with Holm adjustment. Values are expressed per milliliter of cell-free culture supernatant and were not normalized to culture biomass or density

Total protein content also varied markedly among isolates, ranging from 7.67 to 63.38 µg/mL. The highest protein concentration was detected in isolate VAS10 (63.38±0.21 µg/mL), whereas isolate VAS63 showed the lowest protein level (7.67±1.04 µg/mL). However, no clear trend emerged between total protein concentration and antifungal inhibition across isolates. Similarly, Folin–Ciocalteu-reactive phenolic-equivalent content differed substantially among isolates, with values ranging from 3.83 to 12.36 µg GAE/mL. Isolate VAS35 exhibited the highest value, followed by VAS63 and VAS45, indicating variation in this measured trait among the antagonistic isolates.

3.3. Relationship between Antifungal Activity and Biochemical Traits

To examine the statistical relationships between antifungal inhibition and the measured extracellular biochemical traits, Pearson correlation analysis was performed for chitinase activity, total protein content, and Folin–Ciocalteu-reactive phenolic-equivalent content (Figure 2A–C).

Chitinase activity was strongly and positively associated with antifungal inhibition ($r = 0.77$, $p<0.001$; Figure 2A), with higher measured chitinase activity generally occurring in isolates that exhibited greater suppression of *Fusarium* growth. In contrast, total protein content showed only a very weak, non-significant correlation with antifungal activity ($r = 0.14$, $p = 0.596$; Figure 2B), suggesting that overall extracellular protein concentration alone was not a reliable predictor of antifungal efficacy.

Folin–Ciocalteu-reactive phenolic-equivalent content was positively associated with antifungal inhibition ($r = 0.73$, $p = 0.001$; Figure 2C). Among the measured traits, chitinase activity showed the strongest statistical association with antifungal inhibition, followed by Folin–Ciocalteu-reactive phenolic-equivalent content, whereas total protein content showed no significant

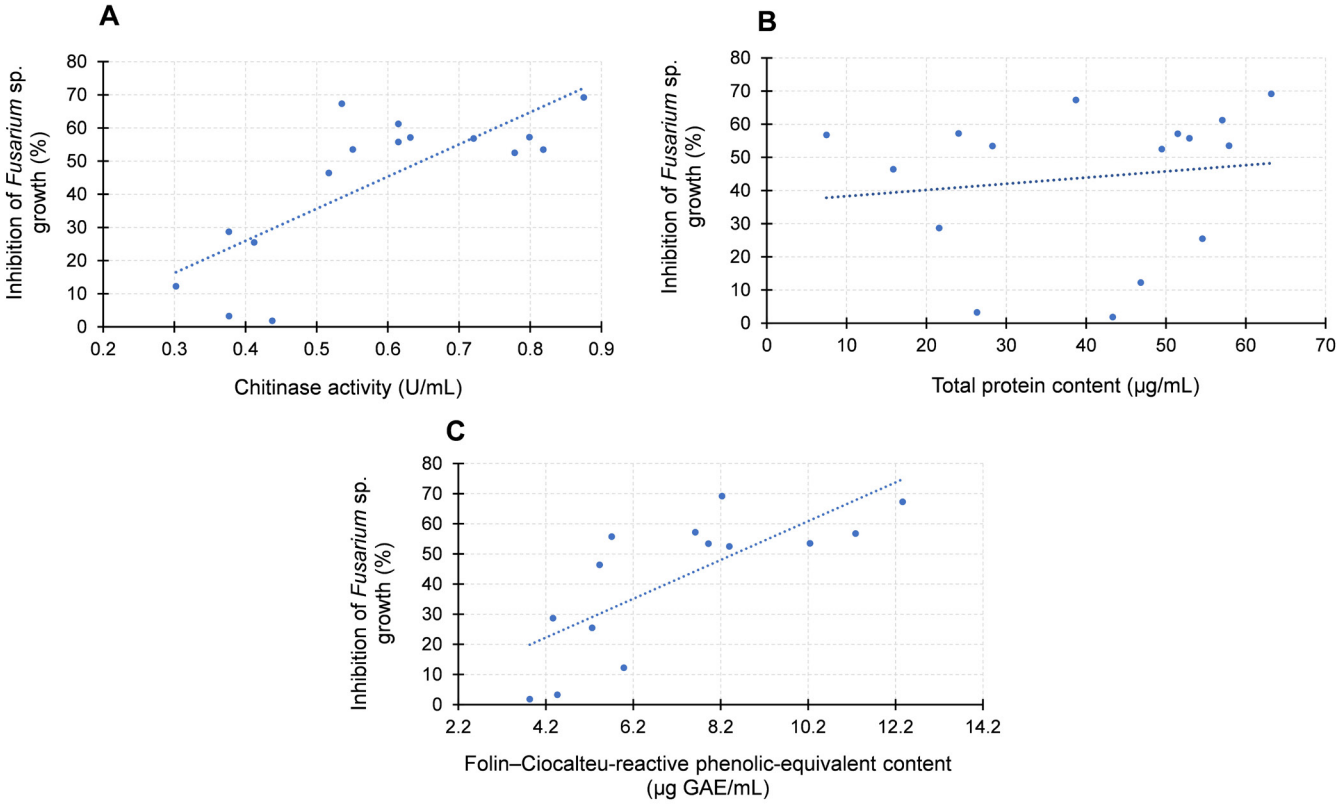


Figure 2. Correlation between antifungal activity against *Fusarium* sp. and biochemical traits of antagonistic *Streptomyces*-like actinomycete isolates: (A) chitinase activity (r = 0.77, p<0.001), (B) protein content (r = 0.14, p = 0.596), and (C) Folin–Ciocalteu-reactive phenolic-equivalent content (r = 0.73, p = 0.001). Dotted lines represent fitted linear regression lines

association. These correlations describe relationships among the measured variables and do not demonstrate causal contributions to antifungal activity.

3.4. Molecular Identification and Phylogenetic Placement of Selected Isolates

Based on their high antifungal activity, we selected isolates VAS10 and VAS35 for molecular identification using 16S rRNA gene sequencing. The 16S rRNA gene sequences of VAS10 and VAS35 were deposited in GenBank under accession numbers PZ770648 and PZ770649, respectively. BLASTn analysis showed that VAS10 exhibited the highest sequence similarities to *Streptomyces globosus* LMG 19896T (99.57%) and *Streptomyces toxytricini* NBRC 12823T (99.56%). VAS35 shared 99.71% sequence identity with several closely related *Streptomyces* strains, including *Streptomyces globosus* LMG 19896T and *Streptomyces toxytricini* NBRC 12823T. Because multiple closely related taxa showed highly similar 16S rRNA gene sequences, BLASTn analysis alone did not allow reliable species-level identification of either isolate (Table 3).

Given the limited discriminatory power of the 16S rRNA gene for resolving closely related species within the genus *Streptomyces* and the high sequence similarity observed, we conservatively assigned both isolates to the genus *Streptomyces* and designated them as *Streptomyces* sp. VAS10 and *Streptomyces* sp. VAS35, respectively. Maximum-likelihood phylogenetic analysis placed VAS10 and VAS35 within a clade containing *Streptomyces globosus* and *Streptomyces toxytricini* (Figure 3). However, the moderate bootstrap support and limited discriminatory resolution of the 16S rRNA gene did not permit reliable species-level assignment.

Representative macroscopic colony and Gram-staining characteristics of *Streptomyces* sp. VAS10 and *Streptomyces* sp. VAS35 are shown in Figure 4. Both isolates formed dry, powdery-to-velvety colonies with visible aerial mycelium on Gause's No. 1 agar. Gram-stained preparations showed Gram-positive, actinomycete-like cellular elements. However, the available light-microscopy preparations could not resolve detailed filament organization and spore-chain morphology. These observations provided

Table 3. BLASTn-based comparison of the 16S rRNA gene sequences of *Streptomyces* sp. VAS10 and *Streptomyces* sp. VAS35 with closely related reference strains

Isolate	Sequence length (bp)	GenBank accession no.	Closest related reference strain	Reference accession no.	Query coverage (%)	Sequence identity (%)
Streptomyces sp. VAS10	1,386	PZ770648	*Streptomyces globosus* LMG 19896^T	NR_042295.1	99	99.57
			Streptomyces toxytricini NBRC 12823^T	NR_112291.1	99	99.56
			Streptomyces amritsarensis 2A^T	NR_126204.1	100	98.99
Streptomyces sp. VAS35	1,364	PZ770649	*Streptomyces globosus* LMG 19896^T	NR_042295.1	100	99.71
			Streptomyces toxytricini NBRC 12823^T	NR_112291.1	100	99.71

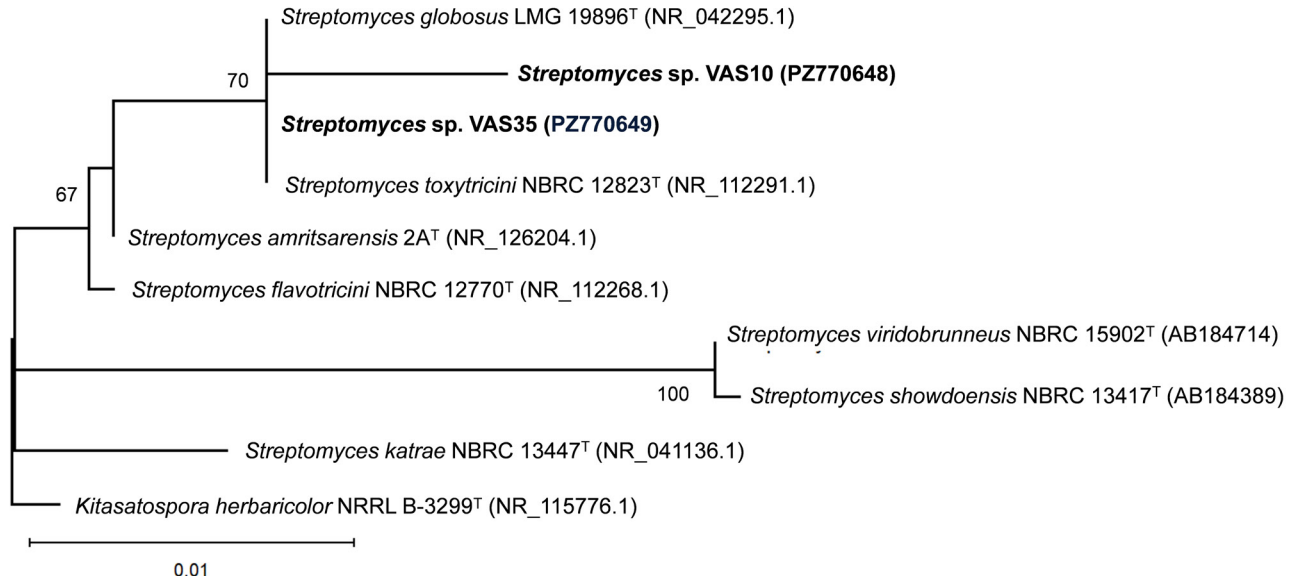


Figure 3. Maximum-likelihood phylogenetic tree based on nearly full-length 16S rRNA gene sequences showing the phylogenetic placement of *Streptomyces* sp. VAS10 (GenBank accession no. PZ770648) and *Streptomyces* sp. VAS35 (GenBank accession no. PZ770649) among closely related Streptomyces reference strains. Multiple-sequence alignment was performed using MUSCLE implemented in MEGA 12, and the phylogenetic tree was reconstructed in MEGA 12 using the Hasegawa–Kishino–Yano model with invariant sites (HKY+I). Branch support values represent bootstrap percentages based on 1,000 replicates; values below 50% are not shown. Kitasatospora herbariicolor NRRL B-3299T (NR_115776.1) was used as the outgroup. The scale bar represents 0.01 nucleotide substitutions per site. The isolates obtained in the present study are indicated in bold

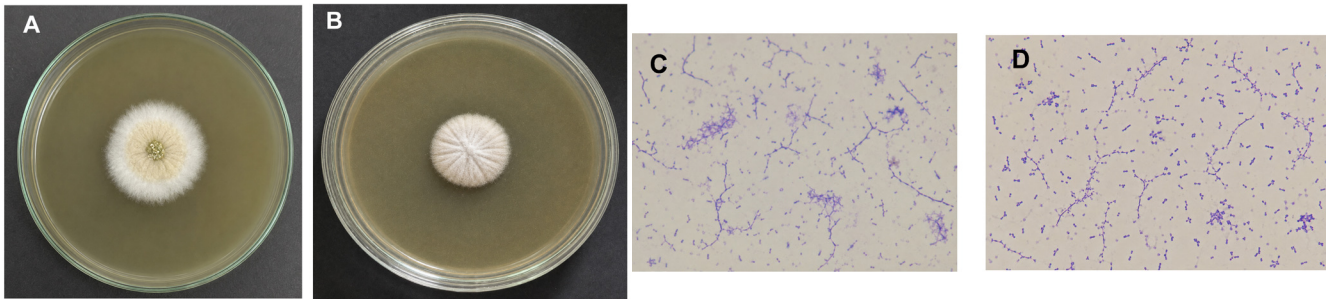


Figure 4. Representative macroscopic and microscopic characteristics of the two selected isolates. (A) Colony morphology of *Streptomyces* sp. VAS10 and (B) *Streptomyces* sp. VAS35 on Gause's No. 1 agar after 96 h of incubation at 28–30°C. (C) Gram-stained preparation of VAS10 and (D) Gram-stained preparation of VAS35 observed using a 100× oil-immersion objective. Both isolates exhibited Gram-positive actinomycete-like cellular elements. Detailed spore-chain morphology was not resolved in the available preparations

preliminary phenotypic support for their classification as *Streptomyces*-like actinomycetes.

4. Discussion

The present study showed that soil-derived actinomycete-like isolates selected based of *Streptomyces*-type colony morphology exhibited substantial variation in in vitro antagonistic activity against *Fusarium* sp. Among the 38 morphologically selected isolates obtained from soil samples, 42% showed antagonistic activity, indicating that antifungal traits were relatively common among the recovered *Streptomyces*-like actinomycete isolates. However, inhibition varied considerably among isolates, suggesting marked functional diversity, consistent with previous reports of strain-dependent antifungal performance in *Streptomyces* species (Khan *et al.* 2023). Under the dual-culture conditions used in this study, *Streptomyces* sp. VAS10 and *Streptomyces* sp. VAS35 exhibited the highest levels of fungal growth inhibition among the tested isolates. Such variability in inhibition capacity has been attributed to differences in secondary metabolite profiles and enzymatic activities among *Streptomyces* strains (Ma *et al.* 2026). This variation supports the use of systematic *in vitro* screening to prioritize isolates for subsequent validation rather than relying on genus-level classification alone (Khan *et al.* 2023). Molecular identification based on BLASTn comparison and maximum-likelihood phylogenetic analysis supported the placement of VAS10 and VAS35 within the genus *Streptomyces*. Both isolates clustered near the *Streptomyces globosus–Streptomyces toxytricini* clade, consistent with their high 16S rRNA gene sequence similarity. We deposited their sequences in GenBank under accession numbers PZ770648 and PZ770649, respectively. Nevertheless, the highly conserved nature of the 16S rRNA gene and the limited phylogenetic separation among closely related *Streptomyces* taxa prevented reliable species-level assignment. Accordingly, the isolates were conservatively designated as *Streptomyces* sp. VAS10 and *Streptomyces* sp. VAS35. Multilocus sequence analysis or genome-based taxonomic approaches would be required for definitive species-level resolution (Komaki 2022; Mispelaere *et al.* 2024). Overall, the combined morphological, 16S rRNA sequence similarity, and phylogenetic evidence supports their genus-level classification and permits comparison with other antagonistic members of Streptomyces (Khan *et al.* 2023).

Selected extracellular biochemical measurements varied among the antagonistic isolates. Chitinase activity showed the closest association with *in vitro* fungal inhibition and may serve as a preliminary screening indicator. Chitin-degrading enzymes have been reported to contribute to fungal antagonism in other experimental systems (Umar *et al.* 2021); however, the present association does not demonstrate that chitinase caused the observed inhibition. The assay measured chitinolytic activity toward colloidal chitin under one defined condition and did not resolve enzyme specificity, isoenzyme composition, or catalytic properties. Folin–Ciocalteu-reactive phenolic-equivalent content was also associated with inhibition; however, this nonspecific assay reflects overall reducing capacity rather than identified phenolic compounds (Dominguez-López *et al.* 2024). Total extracellular protein showed no significant association. These findings support trait-based screening but not a defined biochemical mechanism, and other extracellular products, nutrient competition, and direct microbial interactions may also have contributed (Khan *et al.* 2023).

The present findings should be interpreted in light of several methodological limitations. The extracellular biochemical measurements were obtained at a single harvest point and expressed per milliliter of culture supernatant without normalization to biomass or culture density. Enzyme specificity, extracellular metabolite composition, compound stability, and production kinetics were not assessed. Moreover, the Folin–Ciocalteu assay was nonspecific, and correlation analysis did not establish causality. Consequently, differences among isolates may reflect variation in both culture growth and extracellular production, and the biochemical data provide limited mechanistic insight.

Antifungal activity was evaluated only using an *in vitro* dual-culture assay. Direct antifungal activity of the cell-free supernatants or solvent-derived extracts, minimum inhibitory concentration, spore-germination inhibition, and greenhouse, pot, or field efficacy were not assessed. In addition, the fungal–bacterial confrontation interface was not examined by scanning electron microscopy or high-resolution microscopy; therefore, the present data do not support conclusions about hyphal damage, overgrowth, or mycoparasitism. These endpoints require independent validation.

In conclusion, the present functional screening prioritized *Streptomyces* sp. VAS10 and *Streptomyces* sp. VAS35 for subsequent investigation. Chitinase activity and Folin–Ciocalteu-reactive phenolic-equivalent content were positively associated with *in vitro* antifungal inhibition; however, these relationships do not establish causality. Further studies using cell-free culture supernatants or extracts, metabolite characterization, and in planta assays are required to clarify the underlying antifungal

mechanisms and validate the biocontrol potential of these isolates.

Conflict of Interest

The authors declare no known competing financial interests or personal relationships that could have appeared to influence the work reported in this paper.

Data Availability

The 16S rRNA gene sequences generated for *Streptomyces* sp. VAS10 and *Streptomyces* sp. VAS35 have been deposited in the NCBI GenBank database under accession numbers PZ770648 and PZ770649, respectively.

Acknowledgements

This research is funded by Vietnam National University HoChiMinh City (VNU-HCM) under a project within the framework of the Program titled "Strengthening the capacity for education and basic scientific research integrated with strategic technologies at VNU-HCM, aiming to achieve advanced standards comparable to regional and global levels during the 2025–2030 period, with a vision toward 2045." This work was supported under grant number CB2025-16-08.

References

Amini, J., Agapoor, Z., Ashengroph, M., 2016. Evaluation of *Streptomyces* spp. against *Fusarium oxysporum* f. sp. ciceris for the management of chickpea wilt. *J. Plant Prot. Res.* 56, 10–18. https://doi.org/10.1515/jppr-2016-0038

Bradford, M.M., 1976. A rapid and sensitive method for the quantitation of microgram quantities of protein utilizing the principle of protein-dye binding. *Anal. Biochem.* 72, 248–254. https://doi.org/10.1016/0003-2697(76)90527-3

Davidova, S., Galabov, A.S., Satchanska, G., 2024. Antibacterial, antifungal, antiviral activity, and mechanisms of action of plant polyphenols. *Microorganisms.* 12, 2502. https://doi.org/10.3390/microorganisms12122502

Dominguez-López, I., Pérez, M., Lamuela-Raventós, R.M., 2024. Total (poly)phenol analysis by the Folin-Ciocalteu assay as an anti-inflammatory biomarker in biological samples. *Crit. Rev. Food Sci. Nutr.* 64, 10048–10054. https://doi.org/10.1080/10408398.2023.2220031

Hossain, M.M., Sultana, F., Mostafa, M., Rubayet, M.T., Mishu, N.J., Khan, I., Mostofa, M.G., 2025. Biological management of soil-borne pathogens through tripartite rhizosphere interactions with plant growth-promoting fungi. *Appl. Microbiol.* 5, 123. https://doi.org/10.3390/applmicrobiol5040123

Islam, T., Danishuddin, Tamanna, N.T., Matin, M.N., Barai, H.R., Haque, M.A., 2024. Resistance mechanisms of plant pathogenic fungi to fungicide, environmental impacts of fungicides, and sustainable solutions. *Plants.* 13, 2737. https://doi.org/10.3390/plants13192737

Khan, S., Srivastava, S., Karnwal, A., Malik, T., 2023. *Streptomyces* as a promising biological control agents for plant pathogens. *Front. Microbiol.* 14, 1285543. https://doi.org/10.3389/fmicb.2023.1285543

Komaki, H., 2022. Resolution of housekeeping gene sequences used in MLSA for the genus *Streptomyces* and reclassification of *Streptomyces anthocyanicus* and *Streptomyces tricolor* as heterotypic synonyms of *Streptomyces violaceoruber*. *Int. J. Syst. Evol. Microbiol.* 72, 005370. https://doi.org/10.1099/ijsem.0.005370

Li, Z., He, F., Gai, X., Zhu, H., He, S., Xuan, Y.H., Bai, L., 2025. The growth, development and infection process of the plant pathogen *Fusarium*. *Plant Signal. Behav.* 20, 2573097. https://doi.org/10.1080/15592324.2025.2573097

Ma, X., Jia, C., Su, J., Lu, W., Zheng, R., Yue, S., 2026. Dynamicomic analysis reveals the biocontrol activity of a *Streptomyces avermitilis* SM12 against *Fusarium* spp. *Pestic. Biochem. Physiol.* 216, 106822. https://doi.org/10.1016/j.pestbp.2025.106822

Mispelaere, M., De Rop, A.-S., Hermans, C., De Maeseneire, S.L., Soetaert, W.K., De Mol, M.L., Hulpiau, P., 2024. Whole genome–based comparative analysis of the genus *Streptomyces* reveals many misclassifications. *Appl. Microbiol. Biotechnol.* 108, 453. https://doi.org/10.1007/s00253-024-13290-4

Pacios-Michelena, S., Aguilar González, C.N., Alvarez-Perez, O.B., Rodriguez-Herrera, R., Chávez-González, M., Arredondo Valdés, R., Ascacio Valdés, J.A., Govea Salas, M., Ilyina, A., 2021. Application of *Streptomyces* antimicrobial compounds for the control of phytopathogens. *Front. Sustain. Food Syst.* 5, 696518. https://doi.org/10.3389/fsufs.2021.696518

Palkova, L., Tomova, A., Repiska, G., Babinska, K., Bokor, B., Mikula, I., Minarik, G., Ostatnikova, D., Soltys, K., 2021. Evaluation of 16S rRNA primer sets for characterisation of microbiota in paediatric patients with autism spectrum disorder. *Sci. Rep.* 11, 6781. https://doi.org/10.1038/s41598-021-86378-w

Sarnaik, R., Shelake, J., Waghmare, M., 2025. Fusarium wilt of brinjal: impact, pathogenicity, and sustainable management strategies. *Discover Plants.* 2, 244. https://doi.org/10.1007/s44372-025-00331-z

Subramanian, K., Sadaiappan, B., Aruni, W., Kumarappan, A., Thirunavukarasu, R., Srinivasan, G.P., Bharathi, S., Nainangu, P., Renuga, P.S., Elamaran, A., Balaraman, D., Subramanian, M., 2020. Bioconversion of chitin and concomitant production of chitinase and N-acetylglucosamine by novel *Achromobacter xylosoxidans* isolated from shrimp waste disposal area. *Sci. Rep.* 10, 11898. https://doi.org/10.1038/s41598-020-68772-y

Todorović, I., Moënne-Loccoz, Y., Raičević, V., Jovičić-Petrović, J., Muller, D., 2023. Microbial diversity in soils suppressive to *Fusarium* diseases. *Front. Plant Sci.* 14, 1228749. https://doi.org/10.3389/fpls.2023.1228749

Umar, A.A., Hussaini, A., Yahayya, J., Sani, I., Aminu, H., 2021. Chitinolytic and antagonistic activity of *Streptomyces* isolated from Fadama soil against phytopathogenic fungi. *Trop. Life Sci. Res.* 32, 25–36. https://doi.org/10.21315/tlsr2021.32.3.2

Van der Meij, A., Worsley, S.F., Hutchings, M.I., Van Wezel, G.P., 2017. Chemical ecology of antibiotic production by actinomycetes. *FEMS Microbiol. Rev.* 41, 392–416. https://doi.org/10.1093/femsre/fux005

Zhang, M., Song, Z., Yang, J., Miao, P., Wang, H., Li, H., Wang, J., Kang, Y., 2026. Optimization of fermentation conditions and extracellular metabolic profiling of *Streptomyces rochei* strain W71. *BMC Microbiol.* 26, 77. https://doi.org/10.1186/s12866-025-04652-7